Fault Detection and Identification of Three Phase Overhead Transmission Lines Ended With Underground Cables

تحديد أخطاء خطوط النقل الهوائية المنتهية بكابلات أرضية

A. Elmitwally, S. Mahmoud, and M. H. Abdel-Rahman
Elect. Eng. Dept., Mansoura University,
Mansoura, 35516, Egypt

ملخص

يقترح البحث منظومة لاكتشاف و تحديد الأخطاء فى خطوط النقل الهوائية ثلاثية الأوجه المنتهية بكابلات أرضية، حيث يتم تحديد المقطع الذى به الخطأ عن طريق مربع القيمة الفعالة للفرق بين تيار الوجه الداخل و الخارج من كل مقطع ومقارنتها بحدود عليا يتم تعريفها، و يعين نوع الخطأ بواسطة تحليل الموجات متعدد المستويات لتيار الخطأ عند بداية الخط الهوائى ويحسب مؤشر عبارة عن مجموع القيم المطلقة لمعاملات تحويل الموجات للمستوى الثالث يستخدم كمدخل فى منظومة استدلال بالقواعد تعطى نوع الخطأ،وقد تم التثبت من فاعلية المنهج المقترح بالتطبيق على العديد من حالات الخطأ عند مختلف الظروف.

Abstract

In this paper, a scheme for fault detection and identification of three phase overhead transmission lines ended with underground cables is proposed. Fault detection technique is based on mean square value of the difference between incoming and out going three phase currents of each section. Theses differences are compared against threshold setting values. Faulty phase identification is based on the analysis of three phase currents at one end of transmission line. The transient currents are processed by Discrete Wavelet Transform multi-resolution analysis. In order to find out the faulty phase, the absolute sum of the Wavelet Transform coefficients of the third level detail d3 of each phase current, corresponding to the frequency band 25-12.5 kHz, is computed over one cycle of power frequency. It is used as input to a rule-base system to identify the fault type. Many case studies are provided to validate the proposed algorithm.

1. Introduction

Modern fault classification techniques can be subdivided into several methods. One of the main methods depends on detecting the waveform of currents, voltages, or both of them. This technique depends on fast sampling and monitoring these waveforms prior to and/ or after fault occurrence [1, 2]. In the past, some papers have been reported in the area of waveform distortion, most of them deal with the effect of fault generated transients on the existing protection relays mainly using Fourier analysis [3].

However, Fourier analysis only provides the frequency information and usually losses the time information. Although short time Fourier transform overcomes the time location property, it does not provide multiple resolution in frequency and time, which is a potential feature for analysis signals containing both high and low frequency component together. Wavelet algorithms [4] process data at different scales so that it may provide multiple resolutions in frequency and time, which will mainly, used in this study to classify the faults. Because the original signal or function can be represented in terms of a wavelet expansion using coefficients in a linear combination of the wavelet functions. Wavelet techniques have been successfully applied to many signal and image processing areas, and more recently, several papers have demonstrate the potential applications of wavelets in power system analysis [5,6].

Accepted March 31, 2010.

Fault classification and faulted-phase selection play a critical role in the protection for a transmission line. Identifying the faulted-phase is to satisfy single-pole tripping and autoreclosing requirements [7]. Identifying the type of fault, e.g., single-phase grounding fault, phase-to-phase fault, etc supports the digital relays in order to select different algorithm elements to deal with different fault situations.

In this paper, a scheme for fault detection and identification of three phase overhead transmission lines ended with underground cables is proposed. Fault detection technique is based on mean square value of the difference between incoming and out going three phase currents of each section. Theses differences are compared against threshold setting values. Faulty phase identification is based on the analysis of three phase currents at one end of transmission line. The transient currents are processed by Discrete Wavelet Transform (DWT) multi-resolution analysis using 6-level DWT. In order to find out the faulty phase, the absolute sum of the DWT coefficients of the third level detail d3 of each phase current $S(C_{d3})$, corresponding to the frequency band 25-12.5 kHz, is computed over one cycle of power frequency. $S(C_{d3})$ is given to a rule-base system to identify the fault type. Many case studies are provided to validate the proposed algorithm.

II. Simulated radial system

The system under study is shown in Fig. 1 and it is represented as 220 kV. It consists of three sections, one is transmission line and the others are cables. The ATP/EMTP program is used in this work for modeling the system as below [8].

Fig. 1 Simulated power system

- ***AC. Source***

The source is modeled as a 220 kV sinusoidal A.C voltage source.

- ***Overhead transmission line***

The line consists of a 200 km overhead transmission line. The overhead line is similar to the typical Egyptian 220 kV power line. All relevant data about these lines were offered by the Ministry of Electricity and Energy of Egypt and are given in Fig. 2, and Table 1.

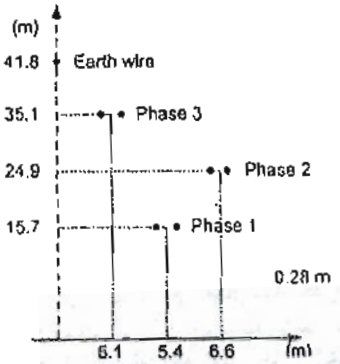

Fig. 2 Overhead line configuration

Table 1 Overhead transmission line data

Number of conductors per phase	2
Diameter of a single conductor	27 mm
Spacing between conductors in the bundle	30 cm
Conductor resistivity	$3.147*10^{-8}$ Ω.m
Earth resistivity	80 Ω.m
Span	360 m

- ***Underground cable***

A 220 kV underground cable of 1500 m length is used. The Bergeron model of the cable is also used. Configurations and installations of the cable line are shown in Fig.3. The physical and insulation constants of each cable phase are identical and its data is given in Table. 2.

Power system simulation is carried out using the ATP/EMTP. The facilities of ATP/DRAW graphic interface and LCC (Line Cable Constants) program are used in order to implement the overhead line transmission line and cables. Bergeron model is used as a quite suitable model for more exact computer simulations

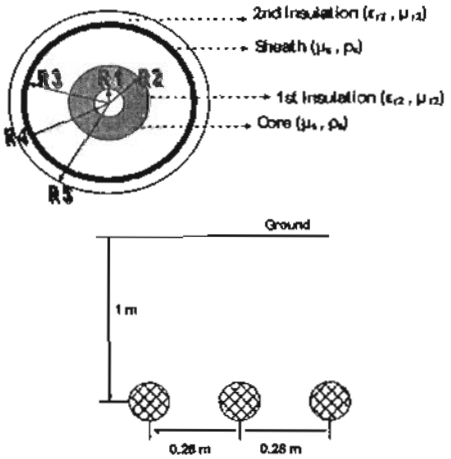

Fig.3 Structure and installation of three phase single core cable

Table. 4.2 Radial cable parameters

R1	0 mm
R2	20 mm
R3	40 mm
R4	43 mm
R5	45 mm
ρ_c	1.742e-8 Ω.m
ρ_s	2.84e-8 Ω.m
ε_r1- ε_r2	2.7
μ_c, μ_r1 , μ_s, μ_r2	1

III. Fault detection

A. Algorithm design

Fig. 4 shows the phase currents measured for single-phase fault case occurring at fault distance of 50 km in the transmission line section depicted in Fig. 1. The waveforms are measured at points m1, m2, m3 and m4.

Applying the current difference for each transmission section in the system shown in Fig.1 can provide a unit protection and therefore the fault event can be detected and the faulty section can be identified. According to this transmission system, Fig.5 shows the flow chart of the fault detection algorithm. Its structure is as follows:

At normal conditions:

1-The 3-phase currents waveforms are measured at points m_1, m_2, m_3 and m_4 of the considered system shown in Fig.1.

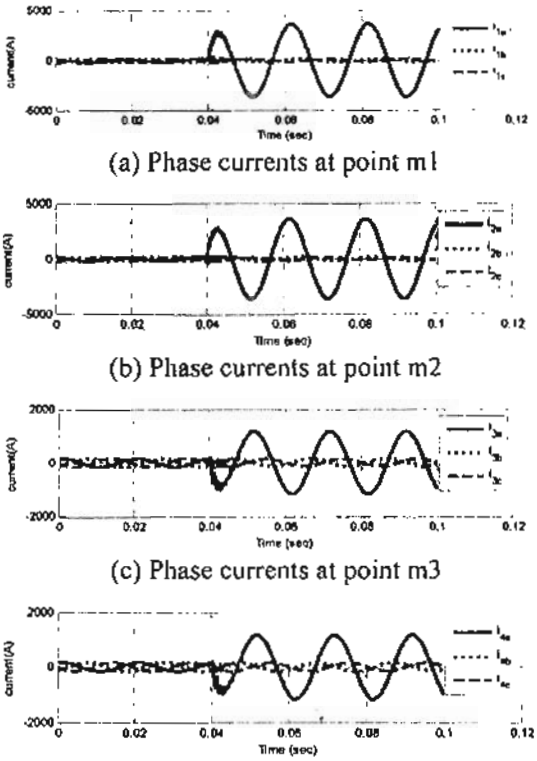

(a) Phase currents at point m1

(b) Phase currents at point m2

(c) Phase currents at point m3

(d) Phase currents at point m4

Fig. 4 Single –phase- to- ground (A-G) fault at 50 km

2- Define the fault detector current settings. It is carried out as follows:

a- Calculate the difference between the incoming and outgoing current signal for each section.

b- Calculate the mean square values of the above current difference signals x_1abc, x_2abc, x_3abc where x_n (a,b,c) are mean square values of the current difference signals of three phase for each section

c- Estimate the normal current difference threshold of the nth section as:

$x_{n\ thresa}=R \times \max(x_n(a,b,c))$

where max $(x_n(a,b,c))$ is the maximum value of the current difference in the three phases of section n. R is a selected scaling up factor.

To process an unknown case:

3- The mean square values of the current difference signals $x_n(a,b,c)$, are determined

as 2.b above.

4- The maximum phase mean square value of the currant difference signals in each section, max($(x_n(a,b,c))$, is compared against the current threshold x_{nthres}

5- If max $(x_n(a,b,c))$ is greater than $x_{n\ thres}$ then the section n is faulty. Otherwise, it is under normal condition.

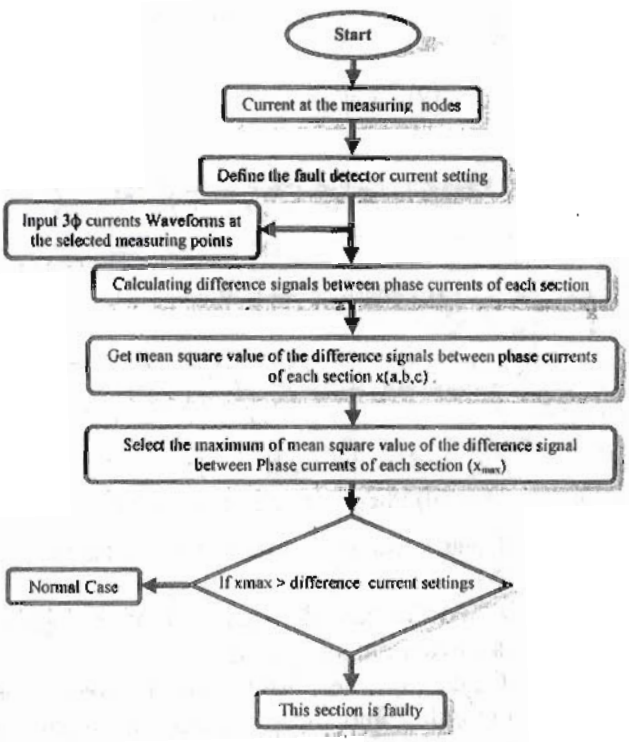

Fig.5 Flowchart for the fault detection technique

When the proposed fault detection algorithm is applied on the measured signals depicted in Fig.4 that is for single line to ground fault (AG) in T.L at 50 km. Calculating the mean square values of the difference between the incoming and outgoing phase currents in each section, it is found as follow:

- For section one, $x_{1a} = 1288.71$, $x_{1b} = 353.45$ and $x_{1c} = 352.94$.
- For section two, $x_{2a} = 6519058.23$, $x_{2b} = 8976.06$ and $x_{2c} = 10241.62$.
- For section three, $x_{3a} = 261.80$, $x_{3b} = 214.60$ and $x_{3c} = 215.788$.

The maximum mean value considering the results of section one is $x_{1a} = 1288.71$, considering section two is $x_{2a} = 6519058.239$ while considering section three is $x_{3a} = 261.80$. By comparing x_1, x_2 and x_3 by $x_{n\ threa} = 10000$, it is found that $x_{1a} < x_{1\ threa}$, $x_{2a} > x_{2\ threa}$ and $x_{3a} < x_{3\ threa}$. Thus, section two is the faulty one.

B. Evaluation of the proposed algorithm

In this section, more evaluation is carried out where the same fault scenarios, (phase-to-ground, phase-to-phase-to-ground, and three - phase faults) respectively, are tested at different fault point along the transmission system with different fault resistances 0, 10, 50, 100 and 1000 Ω. The simulated faults at different points on line as follows:

a- Faults on the left cable (section one)

Fig.6 illustrates the mean squares measured for the three sections considering the (A-G) fault F1 occurring at 40 ms on the left cable. The figure illustrates the values against different fault resistances. Correctly, the algorithm indicates the faulty section as well as the fault phase. The performance is that x_{1a} is greater than the setting while the other mean squares are less than the setting. Such performance is approved up to fault resistance of 900 Ω because the increase of fault resistance results in the decreasing of fault current so more difficulty in fault detection.

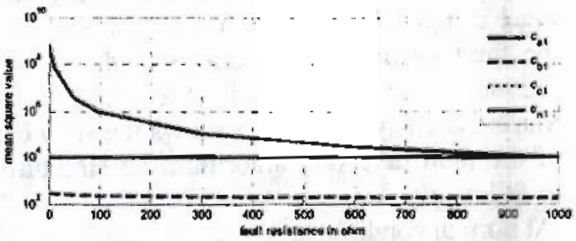

(a) Measurements for the left side cable

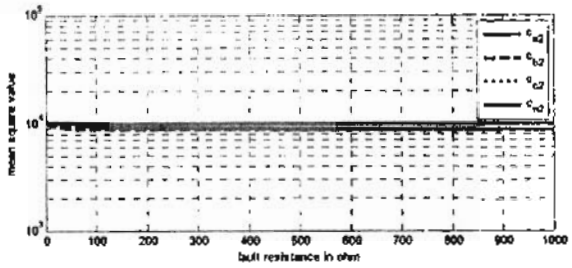

(b) Measurements for the overhead line

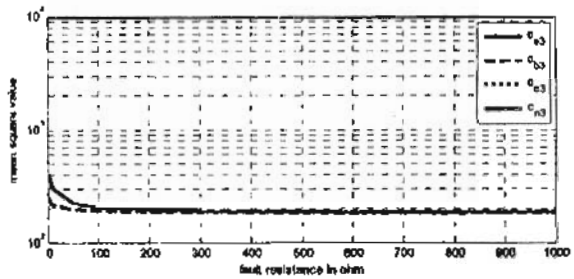

(c) Measurements for cable at right side

Fig.6 Single- phase- to- ground fault (A-G) on the right side cable

b- Faults along transmission line (section two)

For (A-G) fault cases on the overhead line, Fig.7 illustrates the performance of the proposed algorithm. Correctly, the algorithm points out the faulty section 2 and the faulty phase a as x_{2a} is greater than the setting and the other mean squares are under the setting. This performance is confirmed up to fault resistance greater than 1000 Ω.

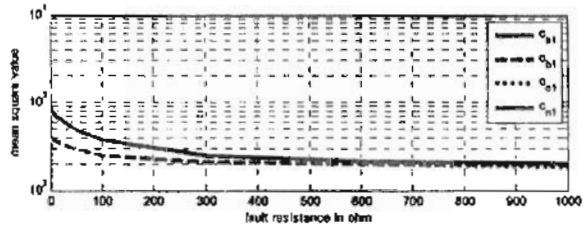

(a) Measurements for the left side cable

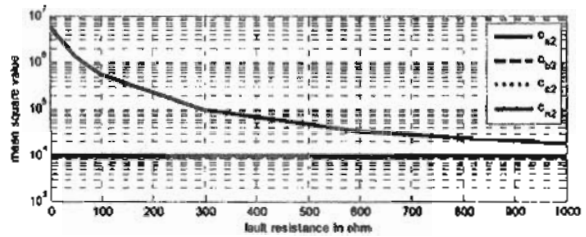

(b) Measurements for the overhead line

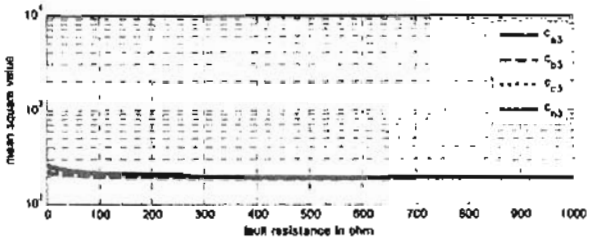

(c) Measurements for the right side cable.

Fig.7. Single- phase-to- ground fault (A-G) on Transmission Line

c- Faults on right cable (section three)

For (A-G) fault cases on the right cable, Fig.8 illustrates the performance. x_{3a} is greater than the threshold setting declaring that the faulty phase a and the faulty section is section three.

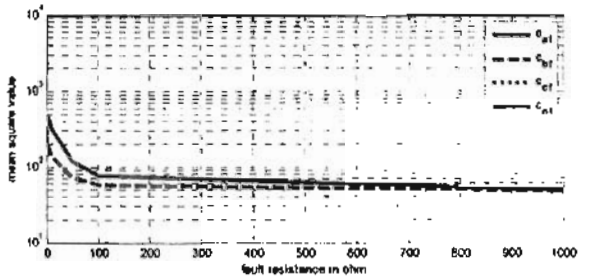

(a) Measurements for the left side cable

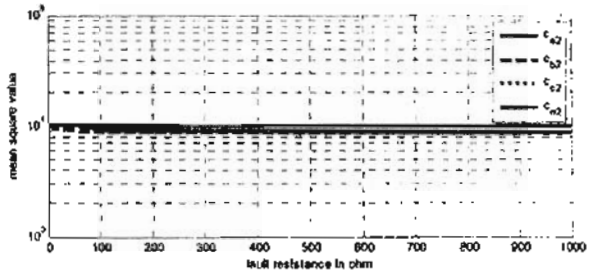

(b) Measurements for the overhead line

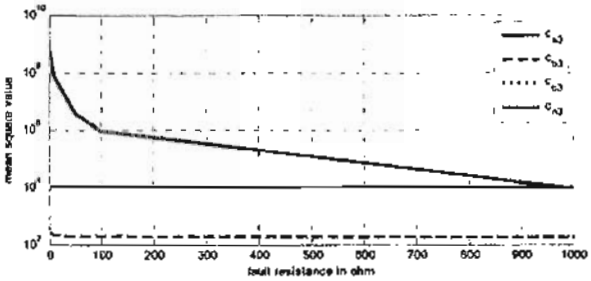

(c) Measurements for the right side cable

Fig.8 Single-phase fault (A-G) at left cable

IV. Fault Identification

A. Algorithm design

In section 3, the fault is detected and the faulty section can be identified using the mean squares of the current differences of each transmission section. However, more study to identify the fault type is carried out by investigating the transients generated due to fault occurrence. Therefore, the DWT is used in order to extract the fault transients and then a proposed algorithm is used to provide a correct decision on the faulty phase.

As aforementioned, the transient currents are extracted by 6-level (DWT) multi-resolution analysis. The choice of mother wavelet is equally important in detecting and localizing different types of fault transients. A commonly used mother wavelet suitable for protection applications is Daubechies wavelet [9], and, for the present work, the db(24) wavelet is used. The current signals are sampled at frequency of 200 kHz, i.e. 4000 sample per cycle.

The zero sequence current is calculated as:

$$i_0 = (i_a + i_b + i_c)/3 \qquad (1)$$

The zero sequence current is also analyzed at 6-level DWT. In order to find out the faulty phase, the absolute sum of the DWT detail d3 coefficients sd3 of each phase corresponding to the frequency band 25-12.5 kHz is computed over the first post-fault one cycle period of power frequency.

The faulty phase (s) is identified as follows:

1. The phase with maximum sd3 (α) is recognized as faulty phase or one of the faulty phases depending on the fault type.
2. The ratio R of α to the sd3 of the other two phases is calculated.
3. The phase with a value of $R > 0.8$ is also recognized as faulty phase. Otherwise, it is a healthy phase.
4. To identify the earth fault, the (sd3) of the zero sequence current i_o $(sd3)_0$ is compared to a selected threshold value ε. If $(sd3)_0 > \varepsilon$, then the case referrers to a ground fault. Otherwise, the case points out to phase fault.

The fault type is identified as fallows:

a. (i) If the number of faulty phases is 3, then the fault is 3-phase fault
   (ii) If the number of faulty phases is only one and $(sd3)_0 < \varepsilon$ then the fault is symmetrical 3-phase fault.
   (iii) If the number of faulty phases is three and $(sd3)_0 > \varepsilon$ then the fault is symmetrical 3-phase-to-ground fault.

b. If the number of faulty phases is only one and $(sd3)_0 > \varepsilon$, then the fault is single phase- to-ground fault.

c. If number of faulty phases is 2, then the fault is phase-to-phase fault
   (i) If $(sd3)_0 > \varepsilon$, then the fault is (phase-to-phase to ground) fault
   (ii) If $(sd3)_0 < \varepsilon$, then the fault is (phase-to-phase) non – ground fault

The sampling rate can be reduced to 100 or 50 kHz, but the used coefficients will be detail d2 or d1, respectively. More reduction in the sampling frequency can be considered, however; the absolute sum detector has less gain [9].

The proposed algorithm to identify the faulty phase(s) can be represented in Flowchart as shown in Fig.9.

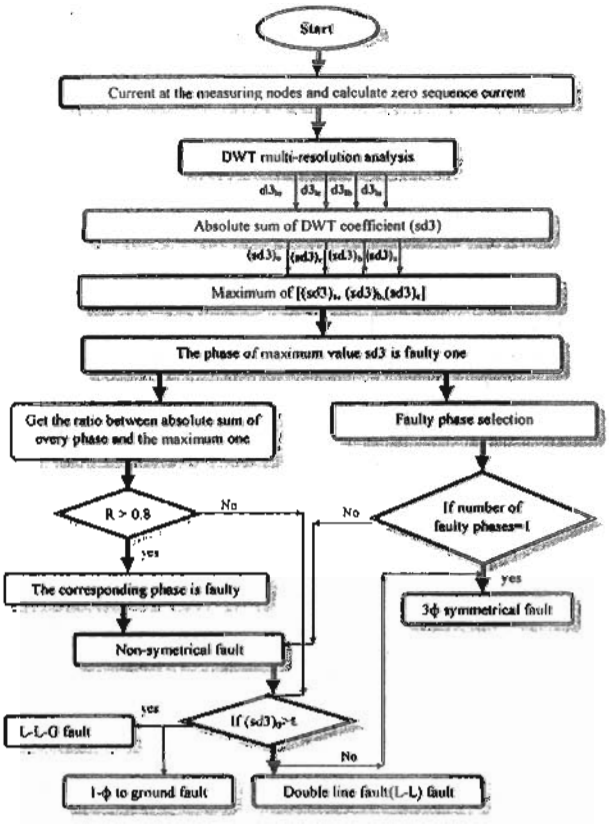

Fig.9 Proposed fault type identification technique

B. Algorithm performance

When the proposed fault identification algorithm is applied on the measured signals depicted in Fig.10. This figure shows the waveforms for single-phase fault (A-G) at L = 10 km. Accordingly, the transients are localized using DWT as shown in Fig.10 b in which they are during one power cycle after the fault occurrence. Calculating the absolute sum detail d_3 coefficient of each phase as in Fig.10 c, it is found that: For phase (a,b,c), $(sd3)_a$ = 1321.36, $(sd3)_b$=729.714, $(sd3)_c$=731.75. The maximum sd3 is $(sd3)_a$= 1321.36. Then it is found that, $R1=(sd3)_b/(sd3)_{max}$= 0.5522 and $R_2=(sd3)_c/(sd3)_{max}$= 0.5538 and $(sd3)_o$= 477.14. Accordingly, the algorithm correctly indicates a-g fault.

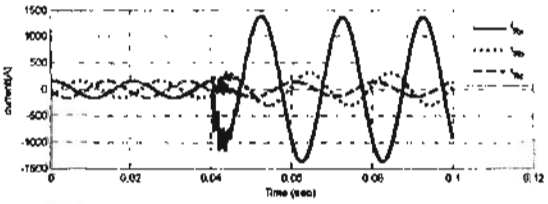

(a) Three phase currents waveforms

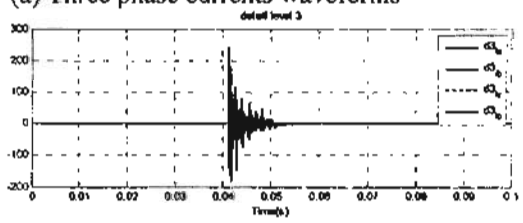

(b) The detail d3 coefficient of each phase

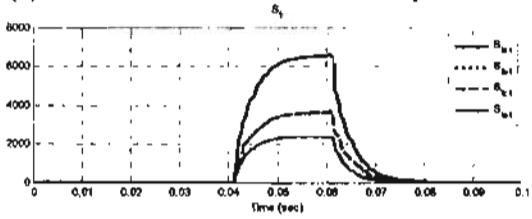

(c) The absolute sum detail d_3 coefficient

Fig.10 Single-phase fault (A-G), L= 10 km, $r_f = 0\ \Omega$.

Similarly, Fig.11 shows the results for A-G ground fault at L= 180 km, $r_f = 0\ \Omega$. The faulty phase has the highest absolute sum when it is compared with the others. Fig.11 shows detail d-3 and sd3 obtained after wavelet decomposition for single-phase-to-ground fault. It can be observed that when fault occurs, it is found that the faulty phase (a) has the highest absolute sum when it is compared with the others. Thus $(sd_3)_a = (sd_3)_{max}$, then maximum absolute sum is phase (a), and R1, R2 have small ratio where $R_1 = (sd_3)_b / (sd_3)_{max}$, $R_2 = (sd_3)_c / (sd_3)_{max}$,$(sd_3)_0 > \varepsilon$, then this fault is a-g.

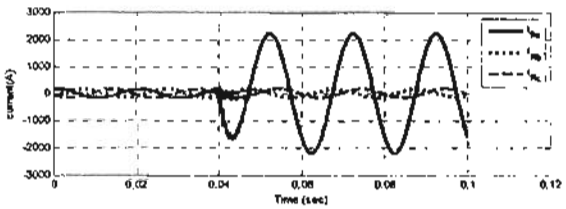

(a) Three phase currents waveforms

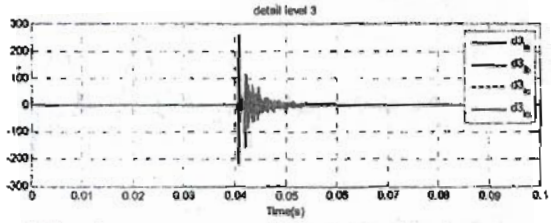

(b) The detail d3 coefficient of each phase

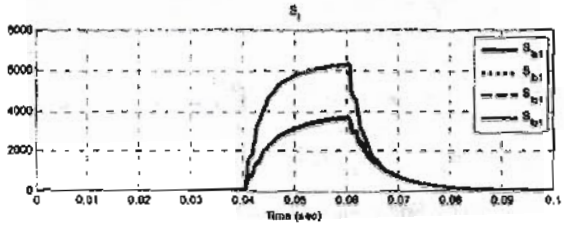

(c) The absolute sum detail d_3 coefficient

Fig. 11 Single- phase fault (A-G), L= 180 km, r_f= 0 Ω.

Fig.12 shows absolute sum of detail d_3 DWT coefficients for double phase fault type. In this figure, $(sd_3)_a = (sd_3)_b = (sd_3)_{max}$ then maximum absolute sum are phase (a,b), and R2 have small ratio where $R_2 = (sd_3)_c / (sd_3)_{max}$,$(sd_3)_0 < \varepsilon$, then this fault is a-b fault type.

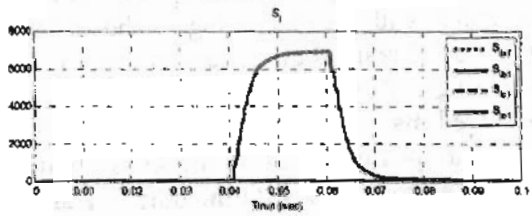

Fig.12 The absolute sum detail d_3 coefficients for double-phase fault in Transmission Line (A-B) at L_f=100 km, r_f= 0 Ω

The proposed fault detection algorithm is evaluated using double- phase-to- ground fault (A-B-G) in T.L at 100 km. Absolute sum of detail d_3 DWT coefficients is depicted in Fig.13. It is found that: for phases (a,b,c), $(sd3)_a$ = 1515.86 , $(sd3)_b$= 1485.09, $(sd3)_c$=377.4 and the maximum sd3 is $(sd3)_a$= 1321.36. $R1=(sd3)_b/(sd3)_{max}$ = 0.97 and $R_2=(sd3)_c/(sd3)_{max}$ = 0.249 and $(sd3)_0$ = 119.27, then this fault ab-g fault.

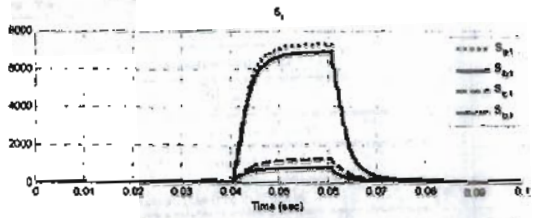

Fig.13 The absolute sum detail d_3 coefficients for double- phase-to ground fault (A-B-G), L_f=100 km, r_f= 0 Ω.

Fig.14 shows absolute sum of detail d_3 DWT coefficients for three- phase-to-ground fault type. In this figure, $(sd_3)_a = (sd_3)_{max}$, and R1, R2 have small ratio where $R_1 = (sd_3)_b / (sd_3)_{max}$, $R_2 = (sd_3)_c / (sd_3)_{max}$,$(sd_3)_0 < \varepsilon$, then this fault is abcg fault.

All above simulated cases ensured that the proposed technique has the ability to identify all fault types.

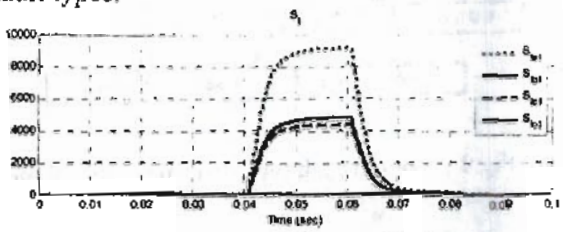

Fig.14 The absolute sum detail d_3 coefficients for three- phase-to-ground fault, L_f= 100 km, r_f= 0 Ω.

C: Response for different fault resistances

Different cases of phase b to ground fault with different fault resistance (0, 10, 50, and 1000Ω) are considered. The results are presented in Figs. 15 to 19. The proposed method is valid in detecting high resistance ground faults on a transmission system.

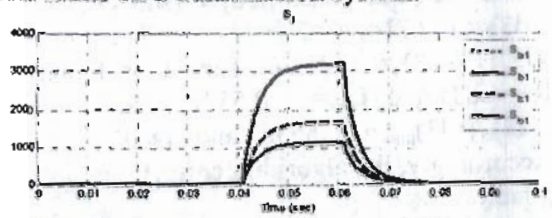

Fig.15 The absolute sum detail d_3 coefficients for single- phase fault (B-G), L_f= 60 km, r_f= 0 Ω.

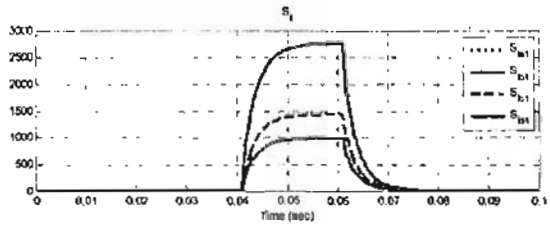

Fig.16 The absolute sum detail d_3 coefficients for single- phase-to-ground fault (B-G), L_f=60 km, r_f=10 Ω

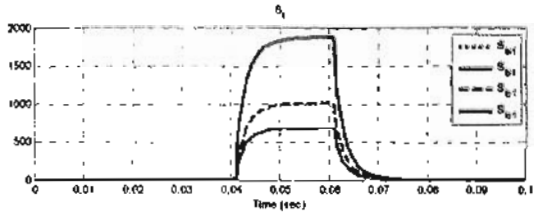

Fig.17 The absolute sum detail d_3 coefficients for single- phase-to-ground fault (B-G), L_f= 60 km, r_f = 50 Ω

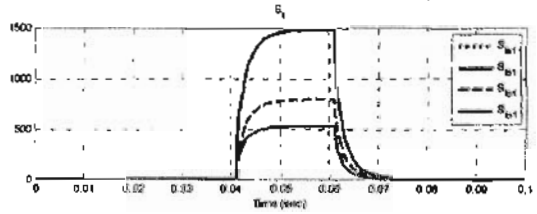

Fig.18 The absolute sum detail d_3 coefficients for single- phase-to-ground fault(B-G), L_f=60km, r_f=100 Ω

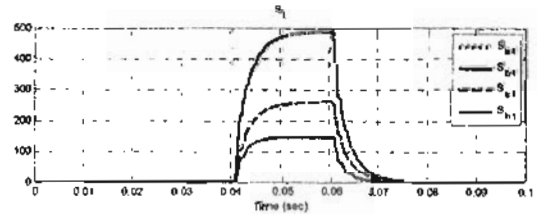

Fig.19 The absolute sum detail d_3 coefficients for single phase fault (phase B), L_f=60 km, r_f= 1000 Ω

V. Conclusion

A scheme for fault detection and identification of three phase overhead transmission lines ended with underground cables is proposed. Fault detection technique is based on mean square value of the difference between incoming and out going three phase currents of each section. Theses differences are compared against threshold setting values. Faulty phase identification is based on the analysis of three phase currents at one end of transmission line. The transient currents are processed by Discrete Wavelet Transform (DWT) multi-resolution analysis using 6-level DWT. In order to find out the faulty phase, the absolute sum of the DWT coefficients of the third level detail d3 of each phase current sd3, corresponding to the frequency band 25-12.5 kHz, is computed over one cycle of power frequency. sd3 is given to a rule-base system to identify the fault type. The proposed scheme has been able to detect and classify all the 11 transmission line fault types for different fault locations and wide range of fault resistance.

VI. References

[1] IEEE Working Group on Estimating the Lightning Performance of Transmission Lines, "IEEE Working Group Report -- Estimating Lighting Performance of Transmission Lines II-Updates to Analytical Models" , IEEE Trans. Power Delivery, Vol. PWRD-8, no. 3,pp. 1254-1267,1993.

[2] M.Kezunovic and B. perunicic,"Automated Transmission Line Fault Analysis Using Synchronised Sampling At Two Ends", IEEE Trans. Power Sys., V.11, NO.1, Feb. 1996.

[3] A. T .Johns, Z.Q.B, Y .H.Song, R.K.Aggarwal", Spectrum Analysis of Fault-Induced Transients For, The Developments of Protection Equipment", IEEE Proc. APSCOM, Singapore, 1993.

[4] A. Graps", An Introduction To Wavelets", IEEE Computer Science Engineering 2, V.2,pp. 50-61, 1995.

[5] S. J. Huang, C. T. Hsieh," High Impedance Fault Detection Utilizing A Wavelet Transform Approach", IEEE Transactions On Power Delivery, V. 14, NO .4, PP. 1401-1410,Oct.1999.

[6] D.C. Robeston, O. I. Camps, J. S. Mayer, W. B. Gish," Wavelet Electromagnetic Power Transients", IEEE Transactions On Power Delivery, V. 11, NO. 2, PP. 1050-1058, April 1996.

[7] N.Elkalashy, M.Lehtonen, H.Darwish, M.Izzularab and A-M.Taalab "DWT-Based Investigation of Phase Currents for Detecting High Impedance Faults Due to Leaning Trees in Unearthed MV Networks" IEEE/PES General Meeting, Tampa, Florida, USA, June 24-28, 2007.

[8] D. Vanhumlen, "Alternative Transient Program", Rule book, EMTP Center, Belgium, 1991.

[9] Raghuveer M .rao and Ajit S. Bopardikar, "Wavelet transforms; introduction to theory and applications, " ADDISON-WESLEY, 2000.